

New cosmic ray electron to positron ratios in the heliosphere

M. S. Potgieter and U. W. Langner

Unit for Space Physics, Potchefstroom for CHE, 2520 Potchefstroom

Abstract. The heliospheric modulation of cosmic rays disguises the true spectral form of the local interstellar spectra for all cosmic ray species below ~ 10 GeV. The lower the energy, the more uncertain they seem to become which is especially true for cosmic ray electrons. Recent modeling of the propagation of cosmic rays through the Galaxy gives the interstellar spectrum for positrons more reliably than before. Using this information, and recent computations of the electron interstellar spectra, the electron to positron ratios are computed with a comprehensive numerical shock-drift modulation model for a simulated heliosphere. These results can be of use for future missions to the outer heliosphere and beyond, and may assist in establishing the local interstellar spectra more accurately for cosmic ray electrons and positrons.

1. Introduction

Drift models predict a clear charge-sign-dependence for the heliospheric modulation of cosmic ray (CR) electrons and positively charged particles due to the different large-scale gradient, curvature and current sheet drifts that charged particles experience in the heliospheric magnetic field (HMF). For example, electrons will drift inwards primarily through the polar regions of the heliosphere during so-called $A < 0$ polarity cycles, that is when the HMF is directed towards the Sun in the northern hemisphere. Positrons, on the other hand, will then drift inwards primarily through the equatorial regions of the heliosphere, encountering the wavy heliospheric current sheet in the process. During the $A > 0$ polarity cycles the drift directions for the two species reverse, so that a clear 22-year cycle is caused (e.g., Burger and Potgieter, 1999). The electron to positron ratios at different energies and positions in the heliosphere can be computed in greater detail if the local interstellar spectra (IS) of the two

cosmic ray species were better known (e.g., Potgieter and Burger, 1990). Recently, new calculations have been published of the IS for CR electrons and positrons that are based on sophisticated models for the propagation of CRs in the Galaxy, and on comparisons with a variety of data sets, including radio synchrotron indices and γ -rays (e.g., Strong et al., 2000; Peterson et al., 1999).

The purpose of this study is to compute the modulation of galactic electrons (e^-) and positrons (e^+) in a simulated heliosphere using these new interstellar spectra as initial values in a modulation drift model with a termination shock (TS) to establish the consequent charge-sign dependence and the affects of the solar wind TS on the modulated e^-/e^+ . For a more elaborated discussion, see Potgieter et al. (2001).

2. Modulation model and parameters

The model is based on the numerical solution of the Parker's (1965) transport equation:

$$\frac{\partial f}{\partial t} = -(V + \langle v_D \rangle) \cdot \nabla f + \nabla \cdot (\mathbf{K}_S \cdot \nabla f) + \frac{1}{3} (\nabla \cdot \mathbf{V}) \frac{\partial f}{\partial \ln R} + Q, \quad (1)$$

where $f(\mathbf{r}, R, t)$ is the CR distribution function; R is rigidity, \mathbf{r} is position, and t is time, with V the solar wind velocity. Terms on the right-hand side represent convection, gradient and curvature drifts, diffusion, adiabatic energy changes and a source, respectively. The latter represents any local heliospheric source, e.g., the Jovian electrons, but for this work all local sources were neglected. The symmetric part of the tensor \mathbf{K}_S consists of a parallel diffusion coefficient (K), and two perpendicular diffusion coefficients ($K_{\perp r}$ and $K_{\perp \theta}$). The anti-symmetric element (K_A) of the tensor describes gradient and curvature drifts in the large scale HMF, with v_D the averaged drift velocity.

The time-dependent transport equation was solved using a shock-drift, modulation-acceleration model with two spatial dimensions, neglecting any azimuthal

dependence (Haasbroek et al., 1997) based on the work of le Roux et al. (1996). The outer modulation boundary was assumed at 120 AU, where the positron IS from Strong et al. (2000) and the electron IS from Langner et al. (2001) were specified. We assume these interstellar spectra to be the local interstellar spectra. A termination shock with a compression ratio of $3.2 < s < 4.0$, and a scale length of $L = 1.2$ AU, was assumed at a position $r_s = 80$ AU. CR particles are therefore subjected to diffusive shock acceleration and drifts at the TS. The solar wind speed V was assumed to change from 400 km.s^{-1} in the equatorial plane ($\theta = 90^\circ$) to a maximum of 800 km.s^{-1} when $\theta \leq 60^\circ$. At the shock, V and B decrease according to le Roux et al. (1996); see also Ferreira et al. (SH3.1, this volume).

The diffusion coefficients K_{\parallel} , $K_{\perp r}$, and K_A are specified respectively as:

$$K_{\parallel} = K_0 \beta f(R) \frac{B_e}{B}; \quad K_{\perp r} = a \frac{K_{\parallel}}{1 + (\lambda_{\parallel} / r_g)^2};$$

$$K_{\perp \theta} = b \frac{K_{\parallel}}{1 + (\lambda_{\perp} / r_g)^2}; \quad K_A = (K_A)_0 \frac{\beta R}{3B}. \quad (2)$$

Here β is the ratio of the speed of the CR particles to the speed of light; $f(R)$ gives the rigidity dependence (in GV); K_0 is a constant in units of $6.0 \times 10^{20} \text{ cm}^2 \text{ s}^{-1}$; a is a constant that determines the value of $K_{\perp r}$, which contributes to perpendicular diffusion in the radial direction, and b a constant that determines $K_{\perp \theta}$ which contributes to perpendicular diffusion in the polar direction. Also, B is the HMF magnitude, with B_e its value at Earth. The ratio $\lambda_{\parallel} / r_g$ is the parallel mean free path to the particle gyro-radius, which should be larger than unity in view of the Bohm limit, $\lambda_{\parallel} = r_g$.

The constants are: $K_0 = 0.5$, $a = 0.4$, $b = 0.6$ and $(K_A)_0 = 0.45$. Diffusion perpendicular to the HMF was enhanced in the polar direction by assuming $b > a$ (see also Kóta and Jokipii, 1995; Burger et al., 2000).

Equation (1) was solved in a spherical coordinate system with the neutral sheet "tilt angle" $\alpha = 10^\circ$, during so-called $A > 0$ (e.g., ~1990 to present) and $A < 0$ (e.g., ~1980 to ~1990) magnetic field polarity epochs. The HMF, assumed to have a basic Parkerian geometry, was modified according to Jokipii and Kóta (1989)

3. Results and discussion

Figure 1(a) shows the electron IS of Langner et al. (2001) and the positron IS of Strong et al. (2000), with the corresponding ratio of the two IS in Fig. 1(b) as a function of kinetic energy. The values were determined by fits to high energy data which are not shown here. The computed electron and positron spectra at different radial distances, as well as the radial profiles at different energies, all in the equatorial plane, are shown in Fig. 2(a) to (d). The computed electron spectra for the $A > 0$ polarity cycle are shown in Fig. 2(a) for 2, 15, 24, 42, 60, 81, 100 and 120 AU, respectively. The modulated electron spectra in the inner heliosphere are compatible with the Ulysses data (Heber, private communication, 1999; Potgieter et al., 1999) above ~500 MeV, but not with the low energy data (≤ 100 MeV). This is understandable because the Jovian electron contribution was not incorporated in the model. However, the same set of parameters gives compatibility with the 16 MeV electron data from Pioneer 10 as shown in Fig. 2(b) for $25 \text{ AU} < r < 50 \text{ AU}$ (Lopate, 1991) and at ~70 AU (Lopate, private communication, 2000). At these radial distances the Jovian electron contribution is considered negligible (Ferreira et al., 2001; Ferreira et al., SH3.1).

The remarkable feature in Fig. 2(a) is that the modulated spectra at large radial distances, above ~500 MeV, exceed the LIS because of the shock acceleration they had experienced before being modulated. The shock effects on the radial dependence of the electrons are also clearly visible, but relatively small at the considered energies. At larger energies the radial dependence beyond the shock may become negative. The corresponding CR positron spectra are shown in Fig. 2(c). The shock-drift effects on these spectra are not as prominent as for the electrons indicating that when the particles drift in over the heliospheric poles, as the positrons do in the $A > 0$ cycle, the shock effects of our model on the modulated spectra are less pronounced. The corresponding radial profiles for the positrons are shown in Fig. 2(d) at energies of 1, 16, 50, 100 and 1000 MeV; the 1 MeV and 1 GeV profiles are clearly distinguishable, but the rest are effectively the same. For the latter, the shock effects are

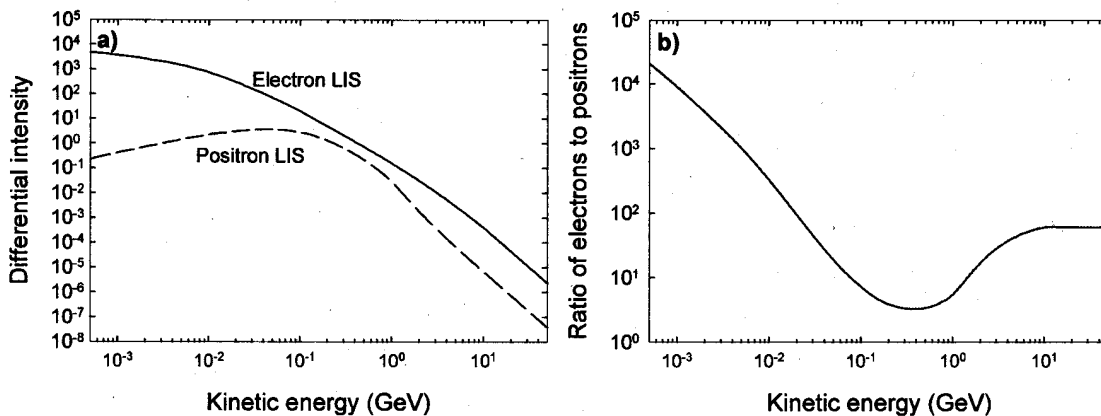


Fig. 1. (a) The electron interstellar spectrum of Langner et al. (2001), and the positron interstellar spectrum of Strong et al. (2000). Differential intensity is in particles $\text{m}^{-2} \text{ s}^{-1} \text{ sr}^{-1} \text{ MeV}^{-1}$. (b) The ratio of the given electron to positron interstellar spectra at 120 AU.

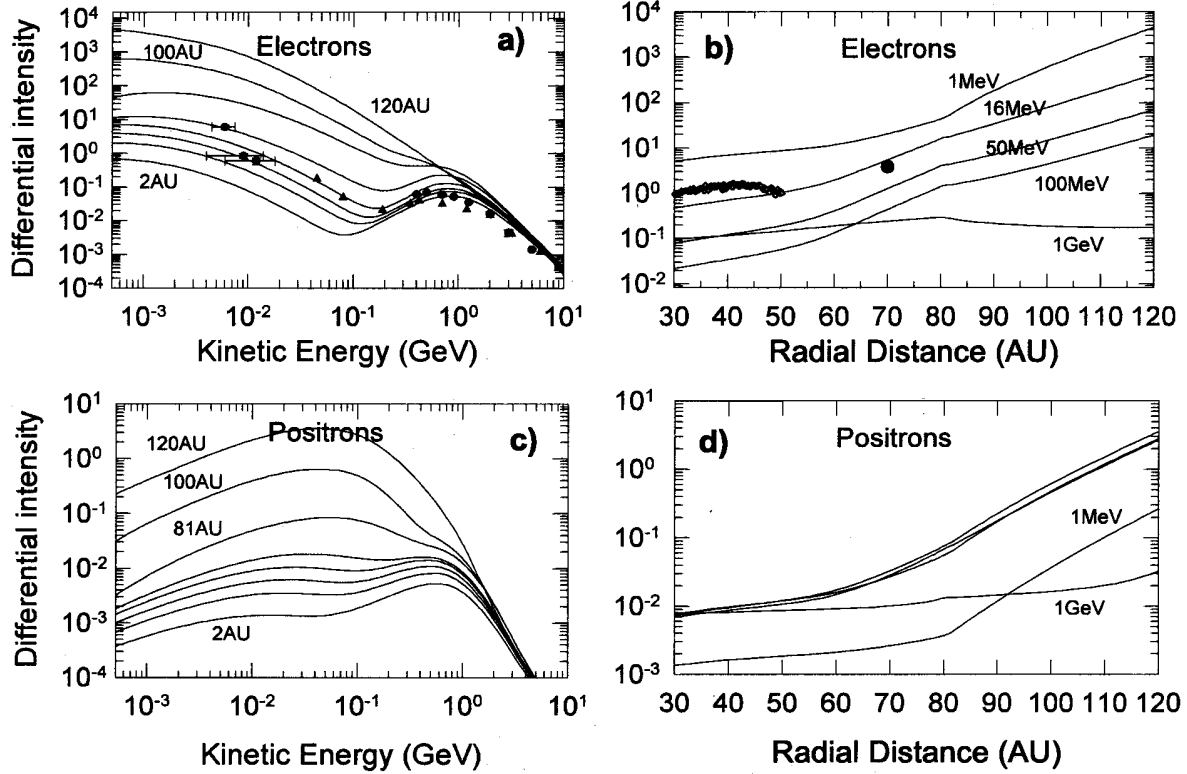


Fig. 2. (a) Computed equatorial spectra for electrons for the $A > 0$ HMF polarity cycle with diffusion coefficients as described in text. Solutions are shown at 2, 15, 24, 42, 60, 81, 100 AU, with the LIS at 120 AU; from bottom to top. The Ulysses data (solid circles) for 1997 at 5 AU (Heber, private communication, 1999; Potgieter et al., 1999), and balloon measurements (solid triangles) for 1977 (Evenson et al., 1983) are shown for comparison. (b) Modulation profiles for 1, 16, 50, 100 and 1000 MeV electrons as a function of radial distance. Data from Pioneer 10 (Lopate 1991; Lopate, private communication, 1999) for 16 MeV electrons are also shown. (c) As in Fig. 2(a), but for positrons, with the LIS at 120 AU. (d) As in (b), but for positrons.

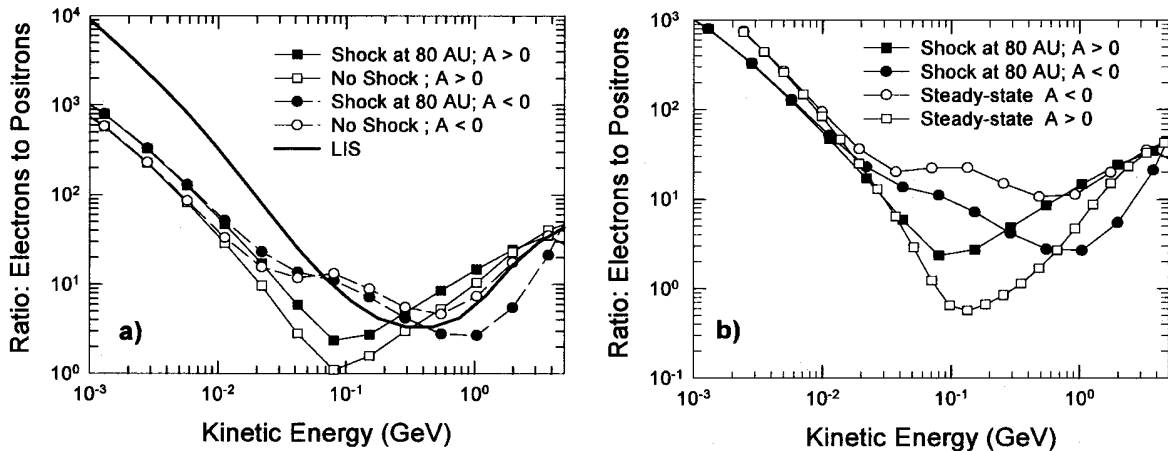


Fig. 3. (a) Ratio of electrons to positrons at 2 AU for the $A > 0$ and $A < 0$ HMF polarity cycles, computed with the TS model with a shock at 80 AU, and without a shock, respectively. The ratio of the two interstellar spectra is shown as a reference at 120 AU. (b) As in (a), but computed with the TS model and a steady-state model, respectively.

barely visible. (See also, Ferreira et al., this volume).

The computations were repeated using the same set of parameters for the $A < 0$ HMF polarity cycle in order to establish if quantitative differences could be found when

compared to what was shown above. That was not the case and the spectra are not shown here. Changing the position of the TS from 80 AU to 100 AU had no significant effect on our computations, except that it

became somewhat easier to find compatibility with the Pioneer 10 data. Computations were also repeated without a TS, but still fully time-dependent, and finally for a steady-state model. Because compatibility with the data at high energies was a criterion, as shown in Fig. 2(a), and with the Pioneer 10 data shown in Figure 2(b), a different set of model parameters had to be used in the steady-state model. In the non-shock model, $(K_A)_0 = 0.7$ had to be used while the rest remained unchanged.

The e^-/e^+ as a function of kinetic energy, computed with the three different model approaches, are shown in Fig. 3(a) at 2 AU for both polarity cycles. They are compared to the IS e^-/e^+ , as a reference. The first important result is that at low energies (< 20 MeV) the e^-/e^+ for both HMF polarity cycles coincides, that is, they become independent of drifts, and second, that this ratio has almost the same slope as the ratio for the IS. (When measured, remember to correct for the Jovian electrons). The differences between the shock and non-shock ratios increase with increasing energy; note how the e^-/e^+ ratios for the $A > 0$ and $A < 0$ cycles have a cross-over at ~ 0.5 GeV, and that this effect is quite pronounced for the TS solutions. In Fig. 3(b) the e^-/e^+ ratios are shown for the TS model and with a steady-state model. In comparison the steady-model clearly gives a maximum charge-sign dependent effect, but without the characteristic cross-over of the TS shock ratios. The ratios are clearly quantitatively different as a function of energy, but note that the slope at low energies (< 20 MeV) is almost the same as for the TS-model ratios despite different sets of diffusion coefficients. Evidently, the steady-state model can be useful as a first order approximation to the TS model (which is considerably more complicated) when studying these aspects, especially at lower energies.

The e^-/e^+ as a function of kinetic energy at different AU are not shown here, but are discussed in detail by Potgieter et al. (2001).

4. Conclusions

Newly computed IS for CR electrons and positrons made it relevant to revisit the computation of the charge-sign dependent effects caused by gradient and curvature drifts in the heliosphere for these species. The purpose of this study therefore was to compute the modulation of CR e^- and e^+ using these new IS and a drift-termination-shock model. The resulting spectra, and the consequent e^-/e^+ as a function of energy, together with the effects of the solar wind termination shock on the modulation of these species, were illustrated in Fig. 1 to 3.

We found the following: (1) At energies below ~ 0.01 GeV, the e^-/e^+ becomes independent of drifts; the energy where this occurs shifts to higher values with increasing radial distances. (2) At these low energies the slope of the e^-/e^+ is insensitive to the values and the energy dependence of the assumed diffusion coefficients (as long as the same set is used for the modulation of both species, of course). (3) Large charge-sign dependence occurs

between ~ 0.02 GeV and ~ 5 GeV in the inner heliosphere. (4) The e^-/e^+ exhibits a characteristic cross-over at ~ 0.3 GeV. This cross-over dissipates with increasing radial distances. Large charge-sign dependence also occurs between ~ 0.2 GeV and ~ 5 GeV in the outer heliosphere. (5) The maximum difference between the ratios for the two polarity epochs shifts to higher energies with increasing distances. (6) Comparing the TS model results with a non-shock model, it was found that the differences between the e^-/e^+ for the two HMF polarity cycles were relatively small although quantitatively the energy dependence differed, especially above ~ 0.2 GeV, due to the absence of re-accelerated low energy cosmic rays.

A comparison of the e^-/e^+ computed with the TS model and a steady state model showed that the steady-model could be useful as a first order approximation to the TS model for CR electron and positron modulation, especially at lower energies. Finally, it is found that the computed e^-/e^+ below ~ 20 MeV exhibits a slope that is almost the same in the inner heliosphere than at the modulation boundary. If good measurements of the two species could be made at Earth, it should be possible to know the ratio of the local interstellar spectra for the two species at these energies from these measurements.

Acknowledgements. We thank Kobus le Roux for making his original shock-drift modulation code available to us, Cliff Lopate for communicating the Pioneer 10 electron observations and Bernd Heber for many helpful discussions.

References

- Burger, R. A. and Potgieter, M. S., *Proc 26th ICRC*, 7, 13, 1999.
- Burger, R. A., Potgieter, M. S., and Heber, B., *J. Geophys. Res.*, 105, 27447, 2000.
- Evenson, P., Garcia-Munoz, M., Meyer, P., Pyle, K. R., and Simpson, J. A., *Astrophys. J.*, 275, L15, 1983.
- Ferreira, S. E. S., Potgieter, M. S., Heber, B., Fichtner, H., Burger, R. A. and Ferrando, P., *Adv. Space Res.*, in press, 2001.
- Haasbroek, L. J., Potgieter, M. S., and le Roux, J. A., *Proc. 25th ICRC.*, 2, 29, 1997.
- Jokipii, J. R. and Kötä, J., *Geophys. Res. Lett.*, 16, 1, 1989.
- Kötä, J. and Jokipii, J. R., *Proc. 24th ICRC.*, 4, 680, 1995.
- Langner, U. W., de Jager, O. C., and Potgieter, M. S., *Adv. Space Res.*, in press, 2001.
- le Roux, J. A., Potgieter, M. S., and Ptuskin, V. S., *J. Geophys. Res.*, 101, 4791, 1996.
- Lopate, C., *Proc. 22nd ICRC.*, 2, 149, 1991.
- Parker, E. N., *Planet. Space Sci.*, 13, 9, 1965.
- Peterson, J. D., Higbie, P. R., Rockstroh, J. M., and Webber, W. R., *Proc. 26th ICRC.*, 4, 251, 1999.
- Potgieter, M. S. and Burger, R. A., *A. & A.*, 233, 598, 1990.
- Potgieter, M. S., Ferreira, S. E. S., Heber, B., Ferrando, P., and Raviart, A., *Adv. Space Res.*, 19(6), 917, 1999.
- Potgieter, M. S., Langner, U. W., and Ferreira, S. E. S., *Adv. Space Res.*, in press, 2001.
- Strong, A. W., Moskalenko, I. V., and Reimer, O., *Astrophys. J.*, 537, 763, 2000.